

# Padé approximation of the $S$ -matrix as a way of locating quantum resonances and bound states

**S. A. Rakityansky<sup>1,2</sup>, S. A. Sofianos<sup>3</sup> and N. Elander<sup>2</sup>**

- 1) *Dept. of Physics, University of Pretoria, Lynnwood Road, Pretoria 0002, South Africa*
- 2) *Dept. of Physics, Stockholm University, Alba Nova University Center, Stockholm, SE-106 91, Sweden*
- 3) *Dept. of Physics, UNISA, Pretoria 0003, South Africa*

September 27, 2018

## Abstract

It is shown that the spectral points (bound states and resonances) generated by a central potential of a single-channel problem, can be found using rational parametrization of the  $S$ -matrix. To achieve this, one only needs values of the  $S$ -matrix along the real positive energy axis. No calculations of the  $S$ -matrix at complex energies or a complex rotation are necessary. The proposed method is therefore universal in that it is applicable to any potential (local, non-local, discontinuous, etc.) provided that there is a way of obtaining the  $S$ -matrix (or scattering phase-shifts) at real collision energies. Besides this, combined with any method that extracts the phase-shifts from the scattering data, the proposed rational parametrization technique would be able to do the spectral analysis using the experimental data.

PACS number(s): 03.65.Nk, 03.65.Ge, 24.30.Gd

Published in: **J. Phys. A: Math. Theor.** **40** (2007) 14857-14869

# 1 Introduction

A full understanding of the properties of a quantum system and prediction of its behaviour cannot be achieved without knowing its spectrum, i.e. the energies of its bound states and resonances. The problems of this kind emerge not only in fundamental research concerning particles, nuclei, and atoms, but also in engineering. For example, modern semiconductor devices based on nano-structures, cannot be properly designed without accurate treatment of various transitions among stationary and quasi-stationary states of the charge carriers (see, for example, Ref.[1] and references therein).

The problem of locating bound states is as old as quantum mechanics itself. Over a century, plenty of exact and approximate methods were developed for solving it. The notion of quasi-stationary states (or quantum resonances) emerged at later stages of the development of quantum mechanics. The attention to such states was drawn by Gamow in his pioneering works on the  $\alpha$ -decay [2].

At the beginning, the development of the methods for locating resonances was hindered by computational difficulties, which are more challenging than that of the bound state problem. The progress in this field was therefore delayed till the advent of modern computers. Another consequence of these difficulties was that the methods for solving the bound and quasi-bound state problems were developed separately despite the fact that the bound and resonant states have essentially the same mathematical nature. Indeed, they correspond to the  $S$ -matrix poles on the complex energy surface at all of which the asymptotics of the solutions of the Schrödinger equation has the same functional form, namely, the outgoing wave. The only difference between bound and quasi-bound states is that the corresponding poles are situated in different domains of the energy surface. As a result, the wave function asymptotics look deceptively different. Being found at real negative energies, the bound state solutions at large distances exponentially decay. However, the decaying exponential function is the same outgoing wave, but taken with pure imaginary momentum that corresponds to a negative energy.

Another fact that makes the kinship between the bound and quasi-bound states apparent, is their mutual transformations. This happens when one increases or decreases depth of the potential. A gradually deepening potential “sucks” the resonances in. The corresponding poles of the  $S$ -matrix move towards the threshold point ( $E = 0$ ) and eventually cross it over to the bound state domain.

Common mathematical ground of the bound and resonant states implies that it should be a unified way of locating them. In quest for such a way most of the modern methods were developed. A review of the existing methods for solving the quasi-bound state problem can be found, for example, in Ref.[3]. One of the new unified approaches not mentioned in that book, is based on a direct calculation of the Jost-function at complex

energies [4] (for references concerning recent development of this method, see also Ref.[5]).

All the methods for locating resonances can be divided in two groups. One of them comprises the approaches, in which all the calculations are done only at real energies. Such methods are rather simple but have limited abilities. They usually fail for wide as well as extremely narrow resonances and are not unified in the abovementioned sense. The other group combines the methods based on locating the  $S$ -matrix poles (or Jost function zeros) on the complex energy surface. These approaches are very powerful, accurate, and unified. The price one has to pay for that is that they require rather sophisticated calculations.

Even the unified complex-energy methods are not fully universal. They are not applicable, for example, to potentials that cannot be analytically continued to complex values of the distance  $r$ . They have difficulties in dealing with energy-dependent and non-local potentials. The methods based on the complex rotation, cannot reach the so-called virtual states that correspond to the  $S$ -matrix poles at negative imaginary momenta, i.e. at negative energies on the unphysical sheet of complex energy surface.

Thus, one can choose either a simple but inaccurate real-energy method or a powerful but complicated complex-energy one. None of them, however, is universal. It would be desirable to have a method that could combine in itself both the simplicity of the real-energy approaches and the power and accuracy of the complex-energy ones. In this paper, we suggest such a method. Besides this, the proposed method is insensitive to the nature of the interaction potential and therefore can be considered as universal.

The idea is based on the fact that two analytic functions coinciding on a curve segment, are identical everywhere in the complex plane (the so-called coincidence principle[6]). Therefore if we calculate (using any appropriate or available method) the  $S$ -matrix along the real positive axis of the energy plane and accurately fit the obtained values with a meromorphic function, for example, with a Padé function, then we can expect that this approximate function will have practically the same singularities at complex energies as the exact  $S$ -matrix. In this way, we can locate the spectral points (bound, virtual, and resonance states) by locating these singularities. In the suggested method, all the poles of the Padé function are located at once, because their coordinates are the fitting parameters and thus they are determined within the fitting procedure.

By constructing the Padé approximant, we actually do an analytic continuation of the  $S$ -matrix from a segment of the real axis, where it is given at a number of discrete points, to complex energies. Similar (but different) procedures in which function values on the complex plane are obtained using the knowledge of its values at a discrete set of real points, were more than once used before and proved to be successful. As an example, we can mention Ref. [7] where a potential  $V(r)$  numerically calculated at a set of real points  $r_1, r_2, \dots, r_N$  was used within a complex rotation method for locating resonances.

Another example is the Padé approximation of the Titchmarsh-Weyl  $m$ -function that was used in Ref. [8] also for locating resonances.

## 2 Rational approximation of the $S$ -matrix

Let us assume that we know the complex-valued function  $S_\ell(k)$  for all real values of the collision momentum  $k \in [0, \infty)$ . Alternatively, we can have the real phase-shift function  $\delta_\ell(k)$  related to the  $S$ -matrix as

$$S_\ell(k) = \exp [i2\delta_\ell(k)] . \quad (1)$$

In practical calculations the interval  $[0, \infty)$  is reduced, of course, to a finite segment  $[k_{\min}, k_{\max}]$  with sufficiently small  $k_{\min}$  and large  $k_{\max}$ , that covers all significant oscillations of the function  $\delta_\ell(k)$ .

We are going to find an approximate function  $\tilde{S}_\ell(k)$  such that the difference  $S_\ell(k) - \tilde{S}_\ell(k)$  is minimal on the segment  $[k_{\min}, k_{\max}]$ . Keeping in mind the well-known fact (see, for example, Ref.[6]) that two analytic functions are identical everywhere if they coincide on a continuous segment, we then expect that the approximate  $S$ -matrix  $\tilde{S}_\ell(k)$  will have almost the same singularities (resonance and bound state poles) as the exact one. The more accurately we approximate the  $S$ -matrix on the real axis, the less different will be the poles of  $\tilde{S}_\ell(k)$  from the corresponding poles of  $S_\ell(k)$ .

There are many ways of approximating  $S_\ell(k)$ . A choice for the functional form of  $\tilde{S}_\ell(k)$  is determined by the fact that it should have simple poles, i.e. at certain points  $k_i$  be proportional to  $\sim (k - k_i)^{-1}$ . Such behaviour is provided by a ratio of two polynomials

$$\tilde{S}_\ell(k) = \frac{a_0 + a_1k + a_2k^2 + \dots + a_Mk^M}{b_0 + b_1k + b_2k^2 + \dots + b_Nk^N} , \quad (2)$$

which in numerical analysis is known as the Padé approximation of the order  $[N, M]$  when the parameters  $a_m$  and  $b_n$  are chosen to reproduce the exact function and all its derivatives up to the order  $M + N$  at  $k = 0$  (see, for example, Refs. [9, 10]).

Here, we will use a special form of the approximation (2). Firstly, we observe that at high energies the  $S$ -matrix tends to unity [11], which can only be achieved if both the numerator and denominator polynomials have the same degree, i.e.  $M = N$ , and  $a_M = b_N$ . Secondly, at zero energy the  $S$ -matrix is unity as well [11], which implies that  $a_0 = b_0$  (without losing the generality, we can assume that  $a_0 = b_0 = 1$ ). Thirdly, the fitting parameters cannot in our case be found using the  $S$ -matrix derivatives, which are not available. Instead, we use the algorithm described next.

### 3 Fitting parameters

To begin with, we re-arrange the polynomials in the form that includes their zeros explicitly, namely,

$$\tilde{S}_\ell(E) = \prod_{n=1}^N \frac{k - \alpha_n}{k - \beta_n} . \quad (3)$$

Knowing some general properties of the  $S$ -matrix, we can simplify the expression (3). This can be done as follows. First of all, we notice that the exact  $S$ -matrix is the following ratio

$$S_\ell(k) = \frac{f_\ell^{(\text{out})}(k)}{f_\ell^{(\text{in})}(k)} , \quad (4)$$

where  $f_\ell^{(\text{in/out})}(k)$  are the Jost functions[12] that are the amplitudes of the incoming and outgoing waves in the asymptotics or the radial wave function,

$$u_\ell(k, r) \xrightarrow[r \rightarrow \infty]{} f_\ell^{(\text{in})}(k)h_\ell^{(-)}(kr) + f_\ell^{(\text{out})}(k)h_\ell^{(+)}(kr) , \quad (5)$$

with the incoming and outgoing spherical waves being represented by the corresponding Riccati-Hankel functions  $h_\ell^{(-)}(kr)$  and  $h_\ell^{(+)}(kr)$ .

Now, we use the fact that  $f_\ell^{(\text{in})}(k)$  and  $f_\ell^{(\text{out})}(k)$  are not independent. Indeed, the incoming and outgoing waves swap their roles when the momentum  $k$  changes its sign and also under the operation of complex conjugation. It is not difficult to show (see, for example, Ref. [12]) that this implies the symmetry properties summarized in Fig. 1. In particular, we have

$$f_\ell^{(\text{out})}(k) = f_\ell^{(\text{in})}(-k) , \quad (6)$$

and thus

$$S_\ell(k) = \frac{f_\ell^{(\text{in})}(-k)}{f_\ell^{(\text{in})}(k)} . \quad (7)$$

This means that not all parameters in Eq. (3) are independent. The numerator polynomial should be the same as the denominator one but taken with negative  $k$ . Therefore

$$\tilde{S}_\ell(k) = (-1)^N \prod_{n=1}^N \frac{k + \beta_n}{k - \beta_n} . \quad (8)$$

As compared to Eq. (3), this not only reduces the number of fitting parameters in half, but also improves the quality of the approximation since the correct structure of the  $S$ -matrix, given by Eq. (7), is taken into account.

The procedure of finding the parameters  $\beta_n$  consists of two stages. At the first stage, we once again re-arrange the polynomials in Eq. (8) to the form (2),

$$\tilde{S}_\ell(k) = \frac{1 + \sum_{n=1}^N a_n k^n}{1 + \sum_{n=1}^N (-1)^n a_n k^n}, \quad (9)$$

where the numerator and denominator are divided by the product  $\beta_1 \beta_2 \cdots \beta_N$ , which gives  $a_0 = b_0 = 1$ . In order to find the parameters  $a_n$ , we multiply Eq. (9) by the denominator of its right hand side and re-write it as

$$\sum_{n=1}^N [1 + (-1)^{n+1} \tilde{S}_\ell(k)] k^n a_n = \tilde{S}_\ell(k) - 1. \quad (10)$$

The last equation, taken at  $N$  different points  $k_1, k_2, \dots, k_N$ , constitutes a system of linear equations

$$\sum_{n=1}^N A_{mn} a_n = B_m, \quad m = 1, 2, \dots, N \quad (11)$$

determining the unknown coefficients  $a_n$ . The matrices of this system are defined as

$$A_{mn} = [1 + (-1)^{n+1} S_\ell(k_m)] k_m^n \quad (12)$$

and

$$B_m = S_\ell(k_m) - 1 \quad (13)$$

with  $S_\ell(k_m)$  being known values of the  $S$ -matrix on the interval  $[k_{\min}, k_{\max}]$ . Therefore, by solving matrix equation (11), we can determine the parameters  $a_n$ .

What we actually need are the  $S$ -matrix poles, i.e. the parameters  $\beta_n$ . So, at the second stage, the parameters  $\beta_n$  are determined as the complex roots of the polynomial

$$P_N(k) = 1 + \sum_{n=1}^N (-1)^n a_n k^n. \quad (14)$$

There are many robust and fast algorithms for finding such roots (see, for example, Ref. [9]).

## 4 Meaningful and spurious poles

What are the mathematical and physical meaning of the poles of the approximate  $S$ -matrix  $\tilde{S}_\ell(k)$ ? As we know, all the poles of the exact  $S$ -matrix are the spectral points, i.e. the bound and virtual states (if any) as well as the resonances. Is this also valid for the poles of  $\tilde{S}_\ell(k)$ ?

At a first sight, it seems that we should give a positive answer to this question. Indeed, the functions  $S_\ell(k)$  and  $\tilde{S}_\ell(k)$  coincide on a segment of the real axis and thus, according to the coincidence principle of the complex analysis, they should be identical everywhere on the complex  $k$ -plane. There are, however, two facts that cast some doubts on this reasoning.

Firstly, the function  $\tilde{S}_\ell(k)$  coincides with  $S_\ell(k)$  not on a continuous segment, but only at a finite number of discrete points  $k_1, k_2, \dots, k_N$ . And secondly, the number  $N$  of these points and thus the number of poles that the function (8) may have, is chosen arbitrarily.

It is natural to expect that the smaller is the difference between  $\tilde{S}_\ell(k)$  and  $S_\ell(k)$  on the chosen segment, the better is the approximation of the  $S$ -matrix at complex momenta. This difference can be made smaller by increasing the number  $N$  of the points, in other words, the number of poles of  $\tilde{S}_\ell(k)$ . Surely, not all of these poles have physical meaning. Some of them may appear at “wrong” places, because of the non-zero difference  $\tilde{S}_\ell(k) - S_\ell(k)$  in between the points  $k_1, k_2, \dots, k_N$ . On the other hand, some of them must be close to the “true” poles, otherwise the approximate  $S$ -matrix would be too different from the exact one.

Those poles of  $\tilde{S}_\ell(k)$  that are close to the “true”  $S$ -matrix poles are meaningful, while all the other poles are spurious. It is obvious that the positions of the meaningful poles are “tied” to the “true” poles, while the spurious poles are “free to move” and appear randomly depending on the choice of the fitting points  $k_1, k_2, \dots, k_N$ .

Therefore, there is a simple way to distinguish meaningful poles from the spurious ones. Indeed, repeating the calculations with different number of fitting points, we can easily find those poles that appear more or less at the same positions. All the other poles should be regarded as spurious. In this way, we can also find an appropriate number  $N$ , with which the meaningful poles converge to the “true” poles within a required accuracy.

When doing the calculations, we found (see the next section) that the spurious poles in many cases appear in symmetric pairs that almost exactly cancel each other in the product (8). For example, if a spurious pole appears at  $k = \beta_n$  then it is accompanied by another pole at  $k = \beta_m$  such that  $\beta_m \approx -\beta_n$ . As a result, in the product (8), we have the factor

$$\frac{(k + \beta_n)(k + \beta_m)}{(k - \beta_n)(k - \beta_m)} \approx 1, \quad (15)$$

which is practically unity everywhere except the immediate vicinity of the spurious poles.

## 5 Numerical examples

The basic idea of the proposed method rests on a rigorous mathematical fact of the identity of two functions that coincide on a continuous curve segment. In numerical calculations, however, we can only guarantee that the exact and approximate functions  $S_\ell(k)$  and  $\tilde{S}_\ell(k)$  coincide at a number of discrete points along the real  $k$ -axis. Of course, after the parameters of  $\tilde{S}_\ell(k)$  are fixed, we can always check how this approximate function reproduces the exact one at the intermediate points. Our hope is based on the well-known fact that rational interpolation of the type (2) works very well even with just few matching points[9]. Certainly, the accuracy of the approximation is best near the matching points and should deteriorate when we move far away into the complex plane.

In order to test how this rational interpolation works in our method, we performed calculations for several well-studied potentials, whose spectral points are known. Since in the proposed method nothing special is associated with the angular momentum, we tested here only the case  $\ell = 0$ . The exact values of the  $S$ -matrix at the fitting points were calculated using the Jost function method described in Ref. [4]. The same method was used to locate the the exact spectral points, with which the approximate  $S$ -matrix poles were compared.

The first of the testing potentials is an exponential well,

$$V_{NN}^{(1)}(r) = -W^{(1)} \exp(-r/R_1) \quad (16)$$

with  $W^{(1)} = 154.06$  MeV and  $R_1 = 0.76$  fm, which roughly describes the  $S$ -wave proton-neutron interaction in the triplet state (total spin = 1). With  $\hbar^2/(2m) = 41.47$  MeV · fm<sup>2</sup> this potential generates a bound state (the deuteron) at  $E = -2.2244674752$  MeV. With  $\ell = 0$ , it does not generate any other poles of the  $S$ -matrix (at least within any physically reasonable domain of the complex plane).

Since there is only one “true” pole, we expect that it is not necessary to have many fitting points in order to reproduce this pole using the Padé approximation. And indeed, starting with just one point, we see a very rapid convergence, so that at  $N = 10$  the exact value of the binding energy is reproduced to eight decimal places, namely, we obtain  $-2.2244674718$  MeV. As the fitting segment for these calculations, we (arbitrarily) chose the interval from  $E_1 = 1$  MeV to  $E_N = 10$  MeV on the real axis. The fitting points,

$$E_n = E_1 + \frac{E_N - E_1}{N - 1}(n - 1), \quad n = 1, 2, \dots, N, \quad (17)$$

were evenly distributed over this interval and the corresponding momenta were taken as  $k_n = \sqrt{2mE_n/\hbar^2}$ . Table 1 shows the meaningful as well as all spurious poles up to  $N = 5$ . It is amazing, but even with only one fitting point we already get a reasonable value for the binding energy.

The second testing potential also describes the  $S$ -wave proton-neutron interaction, but in the singlet state (total spin = 0),

$$V_{NN}^{(0)}(r) = -W^{(0)} \exp(-r/R_0) \quad (18)$$

with  $W^{(0)} = 104.20$  MeV and  $R_0 = 0.73$  fm. It has a weaker attraction and thus, instead of a bound state, it generates a virtual state at  $E = -0.0660644719$  MeV. Similarly to the triplet case, this is the only spectral point in the physically reasonable domain. The convergence here is even more faster (see Table 2, where we show the results up to  $N = 5$ ). With the same choice of the fitting interval and fitting points as we used for the first potential, ten decimal places of the virtual state energy are reproduced already at  $N = 7$ .

The next example is an exponential hump, shown in Fig. 2. It is positive everywhere and therefore can only support resonant states. In the units such that  $\hbar = m = 1$ , the functional form of this potential is

$$V(r) = 7.5r^2 \exp(-r) . \quad (19)$$

The exact  $S$ -matrix corresponding to this potential, has an infinite number of poles forming a string that goes down the  $k$ -plane to infinity. The exact locations of the first nine of these poles are given in Table 3. These values of the resonance energies were obtained using a very accurate method, which is based on a combination of the complex rotation and a direct calculation of the Jost function (see Ref. [4]).

It is naturally to expect that the approximate  $S$ -matrix will reproduce the beginning of the string of resonance poles, i.e. the most significant poles that are close to the real axis and thus to the fitting segment. This is indeed the case as is seen in Figs. 3 and 4. The first of these two figures shows the distribution of the exact and approximate  $S$ -matrix poles over the  $k$ -plane, with the number of fitting points  $N = 20$ . The second figure shows the same, but for  $N = 30$  (few spurious poles that are too far away from the origin are not shown). In both cases the fitting points were uniformly placed on the interval  $1 \leq E \leq 10$ , as is given by Eq. (17). In Figs. 3 and 4, the corresponding points on the real  $k$ -axis are indicated by vertical bars. As is seen, the distances between neighboring bars are decreasing towards the right end of the interval. This is because the relation between  $k$  and  $E$  is not linear.

The poles of the exact  $S$ -matrix are symmetric on the  $k$ -plane relative to the imaginary axis (see Fig. 1). This is a consequence of the Schwartz reflection principle and of the fact that the incoming and outgoing spherical waves swap their roles under the operation of complex conjugation (for proof see, for example, Ref. [12]). The distribution of the Padé poles, shown in Figs. 3 and 4, is almost symmetrical with respect to the imaginary  $k$ -axis, despite the fact that we fitted the  $S$ -matrix only on a short interval on the right hand side of the real axis. This clearly shows that the approximate  $S$ -matrix (8) when fitted to the exact points on that interval, possesses the correct symmetry properties.

Comparing Figs. 3 and 4, we see that, when  $N$  is increased, the meaningful poles converge to the exact ones while the spurious poles change their positions. It is not difficult to design an algorithm for automatically selecting the meaningful poles. Indeed, as is seen, the meaningful are those poles that are located in the fourth quadrant of the  $k$ -plane and do not have a symmetric (or nearly-symmetric) partner at  $-k$  (see Eq. (15) and the associated reasoning).

It should be noted that we did not make any effort to choose the best fitting interval and the best distribution of the fitting points. This is a model case, therefore, when doing the calculations, we already knew the exact positions of the poles and could distribute the points in such a way that the convergence would be much faster. In realistic problems, however, no prior knowledge about resonance energies is available. This is why we chose the fitting points in a sense “arbitrarily”. Despite this, the first few resonances were reproduced to a high accuracy. In Table 4, the exact and approximate  $S$ -matrix poles are compared for the first five resonances generated by the potential (19).

When applying this method to an unknown potential, one should do it in a few iterations. At the first step the fitting interval and points are chosen arbitrarily and the calculations are repeated with different  $N$ . Looking at the results, it is easy to identify possible meaningful poles. If an exact pole is very close to the real axis (extremely narrow resonance) then the corresponding approximate pole at this stage may be found slightly above the real axis. So, the poles that are very close to the real axis but are located above it, should not be excluded at the first iteration.

At the second step, one should choose a fitting interval that covers all “suspected” resonances. If there is a possible narrow resonance, the density of the fitting points should be higher next to it. Repeating the calculations with the adjusted fitting interval, one should be able to obtain the resonance energies and widths of at least few most significant resonances.

A good guidance for choosing the fitting interval and fitting points is the energy (or momentum) dependence of the scattering phase shift  $\delta_\ell(k)$ , if available. Indeed, we are trying to construct such  $\tilde{S}_\ell(k)$  that would be as close as possible to the exact function  $S_\ell(k) = \exp[2i\delta_\ell(k)]$  on the real axis. So, the fitting interval should cover all significant

variations of  $\delta_\ell(k)$ . The density of the fitting points should be high in places where the function  $\delta_\ell(k)$  changes very rapidly, i.e. near narrow resonances.

The  $S$ -wave phase shift function  $\delta_0(k)$  for the potential (19) together with our “arbitrary” choice of the fitting points  $k_1, k_2, \dots, k_N$  are shown in Fig. 5. As is seen, our choice of these points is not the best. They should have been more dense where  $\delta_0(k)$  jumps in  $\pi$  due to the first resonance. We however deliberately stick to the simple set of points evenly distributed over the energy interval  $1 \leq E \leq 10$ . This is done for the purpose of testing the robustness of the method with a poor choice of the fitting points. The results obtained show that even with such a choice the most significant resonances are reproduced rather well. The quality of the approximation of the exact  $S$ -matrix on the fitting interval with  $N = 30$  can be deduced from Fig. 6.

It may seem that one can avoid all this hassle with choosing the fitting points by simply increasing  $N$ . Such an approach, however, is not viable. The problem is that with large  $N$  the linear system (11) becomes ill-conditioned because the neighboring points  $k_n$  and  $k_{n+1}$  are too close to each other and the corresponding equations of the linear system are only slightly different. This is similar to a general and unavoidable problem of fitting functions by high-order polynomials, where one has to solve the so called Vandermonde system, which is ill-conditioned due to the same reason (see Chapter 3 of Ref. [9]). For the potential (19), we found that the instabilities caused by this problem start to show up when there are more than 70 points placed on the interval  $1 \leq E \leq 10$ .

## 6 Conclusion

The proposed method is based on a rigorous mathematical fact that allows us to analytically continue the  $S$ -matrix, known on the real axis, to the domains of complex momentum where it may have poles corresponding to the bound and resonant states, which can thus be easily located. Since the only input information we need, is a table of the  $S$ -matrix values along the real  $k$ -axis, the method is universal, i.e. independent of the nature of the underlying interaction and the way the table is obtained.

The potential can be non-analytic that does not allow using the complex rotation methods. It can be non-local or energy-dependent, which also makes it extremely difficult to apply the rotation. And in principle the  $S$ -matrix table can be obtained from experimental data by means of the phase-shift analysis of the cross section. In all these cases the spectral points can be immediately located as soon as the  $S$ -matrix is calculated for real  $k$ .

The numerical examples show that the proposed method is stable and accurate. With just few matching points, it reproduces the bound states and the most significant reso-

nances to the accuracy that is sufficient for any practical purposes.

## References

- [1] S. A. Rakityansky, Phys. Rev. B **70**, 205323 (2004).
- [2] G. Gamow, Z. Phys. **52**, 510 (1929).
- [3] V. I. Kukulin, V. M. Krasnopolsky and J. Horaček, “*Theory of Resonances*”, Kluwer Academic Publishers, Dordrecht, 1988.
- [4] S. A. Sofianos and S. A. Rakityansky, J. Phys. A: Math. Gen. **30** 3725 (1997).
- [5] S. A. Rakityansky, Phys. Rev. B **68**, 195320 (2003).
- [6] R. P. Boas, “Invitation to complex analysis”, Random House, New York, 1987, page 63.
- [7] S. E. Massen, S. A. Sofianos, S. A. Rakityansky, S. Oryu, Nucl. Phys. A **654**, 597 (1999).
- [8] M. Hehenberger, H. V. McIntosh, E. Brändas, Phys. Rev. A **10**, 1494 (1974).
- [9] W. H. Press, S. A. Teukolsky, W. T. Vetterling, B. P. Flannery, “Numerical Recipes in FORTRAN”, Cambridge University Press, Cambridge, 1992.
- [10] “*The Padé Approximant in Theoretical Physics*”, Edited by G. A. Baker and J. L. Gammel, Academic Press, New York, 1970.
- [11] R. Newton, “*Scattering Theory of Waves and Particles*”, Second Ed., Springer Verlag, New York, 1982.
- [12] J. R. Taylor, “*Scattering Theory*”, John Wiley & Sons, New York, 1972.

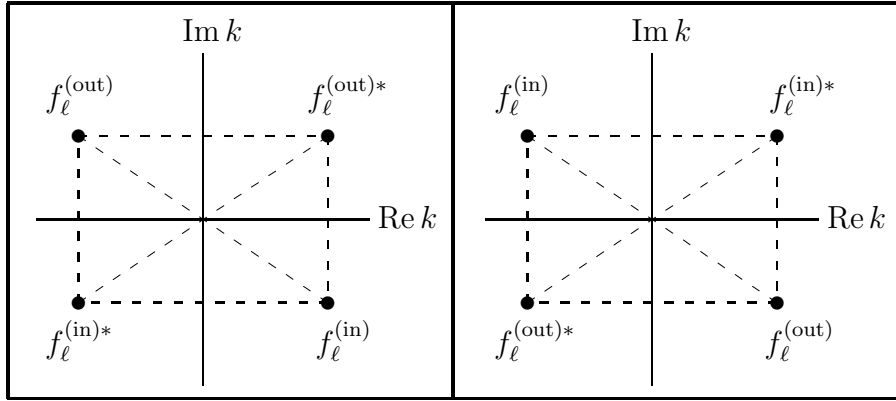


Figure 1: Symmetry properties of the Jost functions on the  $k$ -plane. The dashed lines connect the points at which the values indicated next to them are identical.

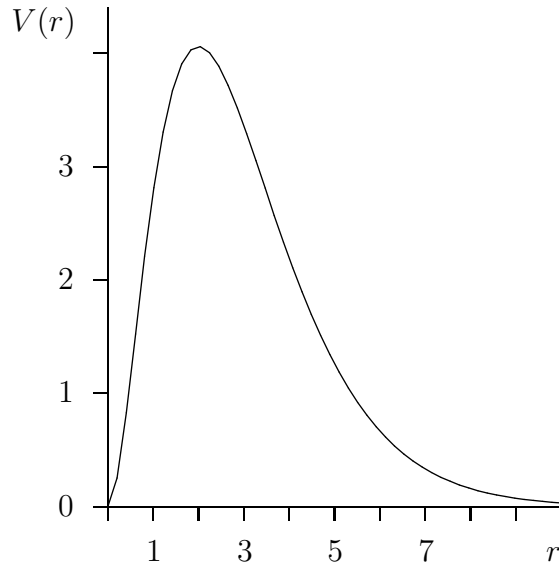


Figure 2: Testing potential (19) in the arbitrary units such that  $\hbar = m = 1$ .

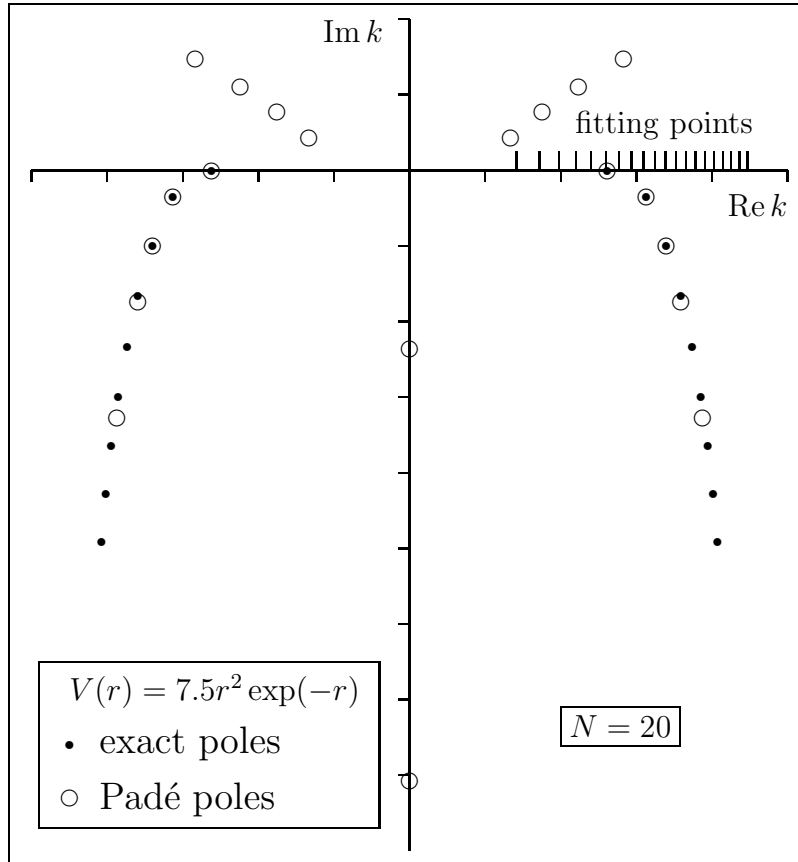


Figure 3: The exact positions of the  $S$ -wave resonance poles (dots) on the momentum plane for the potential (19), and the corresponding poles of the Padé approximation (open circles) obtained with 20 fitting points evenly distributed over the energy interval  $1 \leq E \leq 10$  on the real  $E$ -axis. The corresponding fitting points on the  $k$ -axis are indicated by vertical bars.

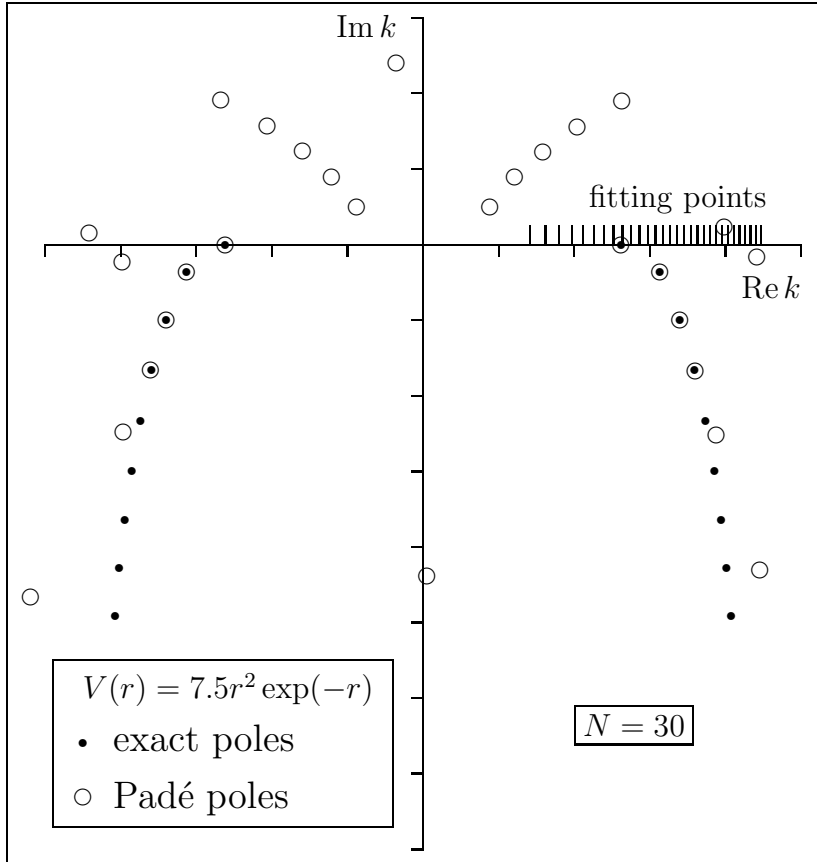


Figure 4: The exact positions of the  $S$ -wave resonance poles (dots) on the momentum plane for the potential (19), and the corresponding poles of the Padé approximation (open circles) obtained with 30 fitting points evenly distributed over the energy interval  $1 \leq E \leq 10$  on the real  $E$ -axis. The corresponding fitting points on the  $k$ -axis are indicated by vertical bars.

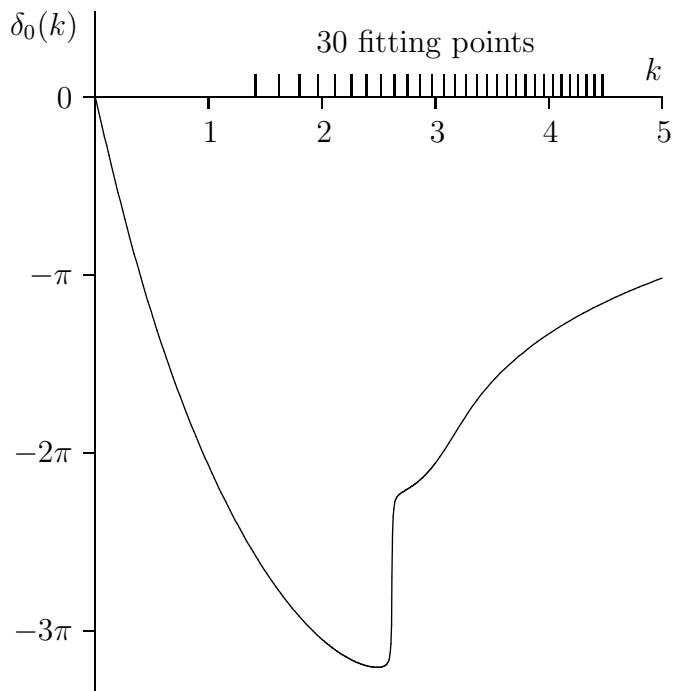


Figure 5: The exact  $S$ -wave phase-shift for the potential (19) as a function of the collision momentum. The vertical bars on the  $k$ -axis show the points  $k_n$ ,  $n = 1, 2, \dots, N$  ( $N = 30$ ) where the exact and the approximate  $S$ -matrices coincide (the Padé fitting points).

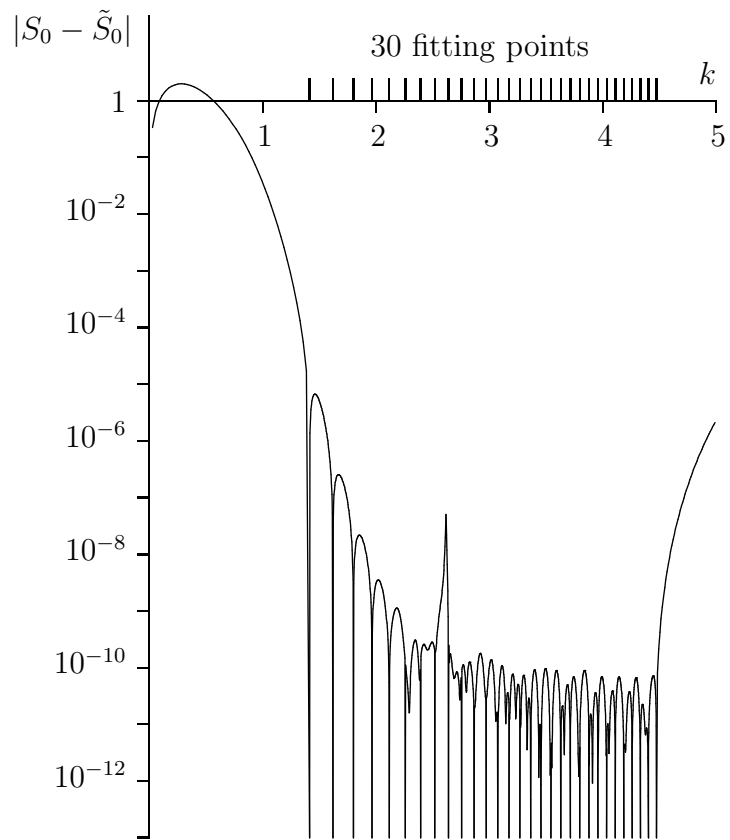


Figure 6: Error in the Padé approximation of the  $S$ -matrix for the potential (19) with 30 points at which the error is zero.

$N$	$\text{Re } k \text{ (fm}^{-1}\text{)}$	$\text{Im } k \text{ (fm}^{-1}\text{)}$	$\text{Re } E \text{ (MeV)}$	$\text{Im } E \text{ (MeV)}$
1	$0.2 \times 10^{-16}$	0.1595408980	<b>-1.0555482734</b>	$0.3 \times 10^{-15}$
2	$-0.6 \times 10^{-16}$	0.9148722594	-34.7100271832	$-0.5 \times 10^{-14}$
	$0.4 \times 10^{-16}$	0.2251639051	<b>-2.1024785800</b>	$0.7 \times 10^{-15}$
3	$-0.1 \times 10^{-12}$	-6.5048412082	-1754.71841570	$0.7 \times 10^{-10}$
	$-0.9 \times 10^{-16}$	0.2305398780	<b>-2.2040739084</b>	$-0.2 \times 10^{-14}$
	$0.3 \times 10^{-14}$	0.7544907890	-23.6070608641	$0.2 \times 10^{-12}$
4	$-0.9 \times 10^{-12}$	1.4615496806	-88.5852061340	-0.0000000001
	$-0.2 \times 10^{-12}$	0.6623217412	-18.1916485831	$-0.9 \times 10^{-11}$
	$0.2 \times 10^{-14}$	0.2315901300	<b>-2.2242014946</b>	$0.4 \times 10^{-13}$
	$0.8 \times 10^{-12}$	-0.9942646075	-40.9956706906	$-0.6 \times 10^{-10}$
5	$-0.2 \times 10^{-10}$	1.3860254952	-79.6666349435	-0.0000000021
	$-0.1 \times 10^{-11}$	0.6586014432	-17.9878555574	$-0.6 \times 10^{-10}$
	$0.4 \times 10^{-14}$	0.2316032946	<b>-2.2244543701</b>	$0.8 \times 10^{-13}$
	$0.8 \times 10^{-11}$	-0.9618425253	-38.3655990692	-0.0000000007
	0.0000000207	-85.5633495380	-303605.468939	-0.0001469872

Table 1: Poles of the approximate  $S$ -wave function  $\tilde{S}_0(k)$ , found for the potential (16) with  $N$  fitting points  $k_1, k_2, \dots, k_N$  evenly distributed over the interval  $1 \text{ MeV} \leq E \leq 10 \text{ MeV}$ . For  $N = 1$ , the single fitting point corresponds to  $E = 1 \text{ MeV}$ . The boldfaced numbers converge to the exact bound-state energy  $-2.2244674752 \text{ MeV}$ .

$N$	$\text{Re } k \text{ (fm}^{-1}\text{)}$	$\text{Im } k \text{ (fm}^{-1}\text{)}$	$\text{Re } E \text{ (MeV)}$	$\text{Im } E \text{ (MeV)}$
1	$-0.2 \times 10^{-16}$	-0.0753661730	<b>-0.2355520897</b>	$0.1 \times 10^{-15}$
2	$-0.8 \times 10^{-16}$	0.7896265828	-25.8569655146	$-0.5 \times 10^{-14}$
	$-0.1 \times 10^{-16}$	-0.0409220958	<b>-0.0694464054</b>	$0.4 \times 10^{-16}$
3	$-0.2 \times 10^{-14}$	0.7187567981	-21.4238720550	$-0.1 \times 10^{-12}$
	$0.2 \times 10^{-16}$	-0.0399961842	<b>-0.0663393412</b>	$-0.8 \times 10^{-16}$
	$0.4 \times 10^{-12}$	-11.9310494904	-5903.25209234	-0.0000000004
4	$-0.9 \times 10^{-12}$	-1.1951630087	-59.2363541815	$0.8 \times 10^{-10}$
	$-0.2 \times 10^{-15}$	-0.0399135508	<b>-0.0660655059</b>	$0.7 \times 10^{-15}$
	$0.6 \times 10^{-13}$	0.6857755943	-19.5028502331	$0.4 \times 10^{-11}$
	$0.1 \times 10^{-11}$	1.4486760697	-87.0315278526	0.0000000001
5	-0.0000005377	-259.016625071	-2782206.21227	0.0115523186
	$-0.5 \times 10^{-10}$	-1.1697429680	-56.7433434047	0.0000000053
	$-0.7 \times 10^{-15}$	-0.0399132475	<b>-0.0660645021</b>	$0.2 \times 10^{-14}$
	$0.2 \times 10^{-11}$	0.6850556465	-19.4619223746	$0.9 \times 10^{-10}$
	$0.9 \times 10^{-10}$	1.4068361606	-82.0769256396	0.0000000102

Table 2: Poles of the approximate  $S$ -wave function  $\tilde{S}_0(k)$ , found for the potential (18) with  $N$  fitting points  $k_1, k_2, \dots, k_N$  evenly distributed over the interval  $1 \text{ MeV} \leq E \leq 10 \text{ MeV}$ . For  $N = 1$ , the single fitting point corresponds to  $E = 1 \text{ MeV}$ . The boldfaced numbers converge to the exact virtual-state energy  $-0.0660644719 \text{ MeV}$ .

$\text{Re } k$	$\text{Im } k$	$E_r$	$\Gamma$
2.6177861703	-0.0048798793	3.4263903101	0.0255489612
3.1300424437	-0.3571442525	4.8348068411	2.2357533377
3.3983924252	-0.9972518977	5.2772798640	6.7781065905
3.5914630921	-1.6639555063	5.0649296074	11.9520695757
3.7383048831	-2.3317810362	4.2688602993	17.4338168679
3.8534573944	-2.9922517758	2.9477816003	23.0610294625
3.9448589582	-3.6424641005	1.1471837383	28.7380142741
4.0173695706	-4.2816627873	-1.0966889789	34.4020435866
4.0742577101	-4.9099759809	-3.7541441225	40.0090149934

Table 3: The  $S$ -wave resonance points,  $k^2/(2m) = E_r - i\Gamma/2$ , of the exact  $S$ -matrix for the potential (19). All the values are given in the arbitrary units such that  $\hbar = m = 1$ . They were obtained using the Jost function method described in Ref. [4].

	$\text{Re } k$	$\text{Im } k$
exact	2.6177861703	-0.0048798793
approximate	2.6177861702	-0.0048798793
exact	3.1300424437	-0.3571442525
approximate	3.1300424420	-0.3571442539
exact	3.3983924252	-0.9972518977
approximate	3.3984191164	-0.9972641751
exact	3.5914630921	-1.6639555063
approximate	3.6001916924	-1.6689691843
exact	3.7383048831	-2.3317810362
approximate	3.8771630790	-2.5129915936

Table 4: Comparison of the first five resonance points for the potential (19), obtained using the rigorous Jost function method [4] (exact) and the Padé approximation with the number of fitting points  $N = 30$  evenly distributed over the interval  $1 \leq E \leq 10$  (the units are such that  $\hbar = m = 1$ ).